The Astrophysical Journal, 667: L9–L12, 2007 September 20

THE FAR-INFRARED LUMINOSITY FUNCTION FROM GOODS-NORTH: CONSTRAINING THE EVOLUTION OF INFRARED GALAXIES FOR $z \leq 1$

Minh T. Huynh,[1] David T. Frayer,[1,2] Bahram Mobasher,[3] Mark Dickinson,[4]
Ranga-Ram Chary,[1] and Glenn Morrison[5]

Received 2007 June 15; accepted 2007 July 30; published 2007 September 11

ABSTRACT

We present the IR luminosity function derived from ultradeep 70 μm imaging of the GOODS-North field. The 70 μm observations are longward of the PAH and silicate features which complicate work in the MIR. We derive far-infrared luminosities for the 143 sources with $S_{70} > 2$ mJy (S/N > 3 σ). The majority (81%) of the sources have spectroscopic redshifts, and photometric redshifts are calculated for the remainder. The IR luminosity function at four redshifts ($z \sim 0.28$, 0.48, 0.78, and 0.97) is derived and compared to the local one. There is considerable degeneracy between luminosity and density evolution. If the evolving luminosity function is described as $\rho(L, z) = (1 + z)^q \rho(L/(1 + z)^p, 0)$, we find $q = -2.19p + 6.09$. In the case of pure luminosity evolution, we find a best fit of $p = 2.78^{+0.34}_{-0.32}$. This is consistent with the results from 24 μm and 1.4 GHz studies. Our results confirm the emerging picture of strong evolution in LIRGs and ULIRGs at $0.4 < z < 1.1$, but we find no evidence of significant evolution in the sub-LIRG ($L < 10^{11}\ L_\odot$) population for $z < 0.4$.

Subject headings: galaxies: evolution — infrared: galaxies

Online material: color figure

1. INTRODUCTION

Deep mid-infrared surveys are revealing a population of mid- and far-infrared luminous galaxies out to $z \sim 3$. These luminous (LIRGs; $10^{11}\ L_\odot < L_{\rm IR} \equiv L_{8-1000\,\mu{\rm m}} < 10^{12}\ L_\odot$) and ultraluminous (ULIRGs; $L_{\rm IR} > 10^{12}\ L_\odot$) infrared galaxies are relatively rare in the local universe, but become increasingly important at high redshift, where dust-enshrouded starbursts dominate the total cosmic star formation rate (e.g., Chary & Elbaz 2001; Blain et al. 2002).

The *Infrared Space Observatory* (*ISO*) showed that infrared luminous starbursts were much more numerous at $z \sim 1$ than at the present time (Franceschini et al. 2001; Elbaz et al. 2002). The *ISO* results were expanded upon by deep surveys at 24 μm with the Multiband Imaging Photometer (MIPS) on the *Spitzer Space Telescope* (e.g., Chary et al. 2004; Papovich et al. 2004). Using the excellent ancillary data in the Great Observatories Origins Deep Survey (GOODS) South and North fields, 15 μm and total infrared luminosity functions were derived from thousands of 24 μm sources (Le Floc'h et al. 2005; Pérez-González et al. 2005). Strong evolution of the IR population was found and the IR luminosity function evolves as $(1 + z)^4$ for $z \lesssim 1$ (Le Floc'h et al. 2005; Pérez-González et al. 2005).

The 24 μm results are dependent on the set of SED templates used to extrapolate the 24 μm flux densities to 15 μm and total infrared luminosities. Furthermore, significant variations in the bolometric correction are expected as strong PAH and silicate emission and absorption features are redshifted into the 24 μm band. Observations with the 70 μm band of MIPS are closer to the peak in FIR emission and are not affected by PAH or silicate features for $z \lesssim 3$. They should therefore provide more robust estimates of the far-infrared (FIR) luminosities.

Studies by *ISO* in the FIR regime have been limited in sensitivity ($S_{90\,\mu{\rm m}} \gtrsim 100$ mJy, $S_{170\,\mu{\rm m}} > 200$ mJy) and redshift completeness (Serjeant et al. 2004; Takeuchi et al. 2006). Frayer et al. (2006a) derived a FIR luminosity function (LF) for the Extragalactic First Look Survey (xFLS) from *Spitzer* 70 μm data, but this survey had incomplete redshift information at faint fluxes, and it was limited to $z < 0.3$ and bright ($S_{70\,\mu{\rm m}} \gtrsim 50$ mJy) sources. In this Letter we present the infrared luminosity function up to redshift 1 from the ultradeep 70 μm survey of GOODS-N.

We assume a Hubble constant of 71 km s^{-1} Mpc^{-1}, and a standard ΛCDM cosmology with $\Omega_M = 0.27$ and $\Omega_\Lambda = 0.73$ throughout this Letter. We define the IR flux as the integrated flux over the wavelength range 8–1000 μm.

2. THE DATA

2.1. *Ultradeep* 70 μm *Imaging*

The GOODS-N field is centered on the Hubble Deep Field–North at $12^{\rm h}36^{\rm m}55^{\rm s}$, $+62°14'15''$. The MIPS 70 μm observations of GOODS-N were carried out during Cycle 1 (*Spitzer* program ID 3325; Frayer et al. 2006b) and Cycle 3 (2006 January) for the Far Infrared Deep Extragalactic Legacy project (FIDEL; *Spitzer* PID: 30948, PI: Dickinson). Together these data map a region $10' \times 18'$ to a depth of 10.6 ks.

The raw data were processed off-line using the Germanium Reprocessing Tools (GeRT), following the techniques described in Frayer et al. (2006b). We have cataloged 143 sources (over $\sim$185 arcmin^2) with $S_{70} \gtrsim 2.0$ mJy (S/N > 3 σ) in GOODS-N. The 70 μm images have a beam size of 18.5″ FWHM, and in the presence of Gaussian noise the 1 σ positional error of sources is of order $0.5\theta_{\rm FWHM}$/(S/N), i.e., 3″ for the faintest sources.

[1] *Spitzer* Science Center, MC 220-6, California Institute of Technology, Pasadena, CA 91125; mhuynh@ipac.caltech.edu.
[2] NASA *Herschel* Science Center, IPAC, MC 100-22, California Institute of Technology, Pasadena, CA 91125.
[3] Space Telescope Science Institute, 3700 San Martin Drive, Baltimore, MD 21218.
[4] National Optical Astronomy Observatory, P.O. Box 26732, Tucson, AZ 85726.
[5] Institute for Astronomy, University of Hawaii, Honolulu, HI 96822; and Canada-France-Hawaii Telescope, Kamuela, HI 96743.

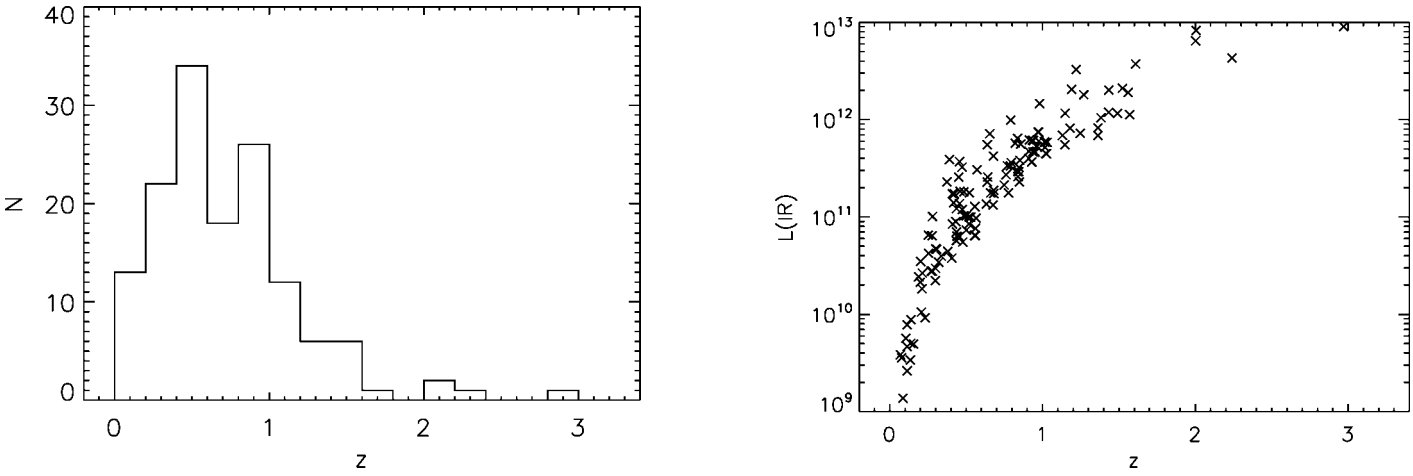

FIG. 1.—*Left*: Redshift distribution of the 70 μm sources. *Right*: IR luminosity (in $L_{\odot}$) vs. redshift for the 70 μm sources.

2.2. *Redshifts*

All 70 μm sources were matched to 24 μm and IRAC sources to obtain good positions. The best *Spitzer* position was then used to search for optical redshifts. About 7% of the 70 μm sources have more than one 24 μm source within the 70 μm beam, and these were deblended individually (e.g., Huynh et al. 2007). Spectroscopic redshifts are available for 116 of the 143 objects (Cohen et al. 2000; Wirth et al. 2004; D. Stern et al. 2007, in preparation).

Photometric redshifts were derived for 141 of the 143 sources with the extensive photometry available: *HST* ACS (Giavalisco et al. 2004), *U*- (NOAO), *BVRIz*- (Subaru-SupremeCam), and *JK*- (NOAO/Kitt Peak–Flamingo) band imaging. The photometric redshifts were calculated using the $\chi 2$ minimization technique as explained in Mobasher et al. (2007). We have photometric redshifts for 26/27 sources that do not have a spectroscopic redshift and we therefore have redshift information for 142/143 sources.

We quantified the reliability of the photometric redshifts by examining the fractional error, $\Delta \equiv (z_{\rm phot} - z_{\rm spec})/(1 + z_{\rm spec})$. For all 115 70 μm sources with both photometric and spectroscopic redshifts, we found that the median fractional error, Δ, is 0.012 ± 0.20. Assuming that the six cases where the fractional error is greater than 0.2 are outliers, the success rate of the photometric redshift method is 95%. Removing the six outliers gives a median fractional error of 0.0014 ± 0.05. We therefore conclude that the photometric redshifts are statistically reliable.

The 70 μm sources have a median redshift of 0.64 (see Fig. 1). The majority (79%) of sources lie at $z < 1$, as expected for the survey sensitivity and steep *k*-correction that is present at 70 μm.

3. INFRARED LUMINOSITIES

Many authors argue that the MIR is a good indicator of the bolometric IR luminosity for normal and IR luminous galaxies (e.g., Chary & Elbaz 2001). Based on this, several authors have developed sets of galaxy templates that can be used to estimate the total infrared luminosity (Chary & Elbaz 2001; Dale & Helou 2002; Lagache et al. 2003).

We use the luminosity-dependent SED templates based on local galaxies from Chary & Elbaz (2001) to determine the IR luminosities of the 70 μm galaxies. However, it is not clear whether local templates can accurately reproduce the MIR SED of distant galaxies because PAH and silicate absorption features are dependent on complex dust physics, including the intensity of the radiation field, the metallicity of the ISM, and the distribution of grain sizes. For this reason we determine the IR luminosities of the 70 μm galaxies by fitting templates to the observed 70 μm flux density only, which is longward of the PAH and silicate features.

The IR luminosities as a function of redshift are shown in Figure 1. Most of the sources below redshift $z = 1$ have LIRG-like luminosities. The higher redshift sources are luminous ULIRGs with possibly an embedded AGN.

The estimated accuracy of the IR luminosity, from the 70 μm flux density calibration and PSF fitting errors alone, is 9%. However, the luminosities derived are dependent on the SEDs used. The adopted template SEDs do not reflect the full range of SEDs observed in galaxies, and thus are the main source of systematic errors. For example, the total IR luminosity derived from the MIR regime can vary by a factor of 5 for local galaxies (Dale et al. 2005). We are working longward of the PAHs and silicate features which affected previous work based on the MIR, but, on the other hand, the rest-frame wavelengths probed at 70 μm are affected by dust temperatures and emissivity.

To test the consistency of our derived IR luminosities and the application of the adopted SEDs, we use the well-known FIR-radio correlation. The deep radio image of GOODS-N (5 μJy rms at 1.4 GHz; G. Morrison et al. 2007, in preparation) detects 120/143 (84%) of the 70 μm sources at 3 σ or above. The FIR-radio correlation, $q = \log({\rm FIR}/S_{1.4\ {\rm GHz}})$, where "FIR" here refers to the flux between 40 and 120 μm (e.g., Yun et al. 2001), has an observed local value of $q = 2.34 \pm 0.3$ (Yun et al. 2001). Adopting an average factor of 2.0 between IR and FIR (e.g., Dale & Helou 2002) and a radio spectral index of $\alpha = -0.8$,[6] we find $q = 2.2 \pm 0.2$ for the radio detected sources. Including the 24 μm data in the fits to the SEDs gave a slightly larger dispersion in q. This suggests that the IR luminosities as estimated from the 70 μm data alone are reasonable.

4. INFRARED LUMINOSITY FUNCTIONS

In this section we explore the evolution of the IR luminosity function between redshifts 0 and 1.

[6] $S_{\nu} \propto \nu^{\alpha}$.

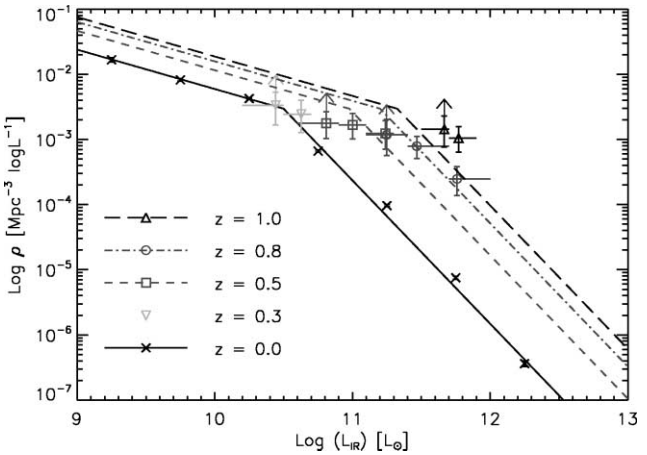

FIG. 2.—IR luminosity function (LF). Crosses mark the local LF from Sanders et al. (2003), and the corresponding solid line is the double-power-law fit to the local data. The symbols mark the LF calculated in this work at redshift 0.3 (*upside-down triangles*), 0.5 (*squares*), 0.8 (*circles*), and 1.0 (*triangles*). The lines are the local LF evolved to the corresponding redshift with the best-fit pure luminosity evolution parameters. The arrows indicate bins which are incomplete because of the survey sensitivity. The horizontal error bars indicate the bin sizes. [*See the electronic edition of the Journal for a color version of this figure.*]

4.1. *Methodology*

The luminosity functions were derived for four redshift bins, $0.2 < z < 0.4$, $0.4 < z < 0.6$, $0.6 < z < 0.9$, and $0.9 < z < 1.1$, using the usual $1/V_{\rm max}$ method (Schmidt 1968). These redshift bins were made wide enough so that there is a reasonable number of sources for calculating the luminosity function. The bins have median redshifts of 0.28, 0.48, 0.78, and 0.97, so a moderate range in redshift is explored. The comoving volume for each source is $V_{\rm max} = V_{z_{\rm max}} - V_{z_{\rm min}}$, where $z_{\rm min}$ is the lower limit of the redshift bin, and $z_{\rm max}$ is the maximum redshift at which the source would be included in the catalog, given the limiting 3 σ limit, or the maximum redshift of the bin.

As mentioned in § 2.2, we have almost complete redshift information on the 70 μm sample. A correction factor for each individual source was computed to correct for source detectability across the full image and flux boosting (i.e., the overestimation of the flux densities of low-S/N sources). This correction was calculated using the Monte Carlo approach described by Chary et al. (2004), and it is the same correction applied to the source counts (Frayer et al. 2006b).

4.2. *Results and Discussion*

The luminosity functions were derived from the rest-frame IR μm luminosities. In Figure 2 we plot the luminosity functions for the redshift bins explored, and the data are summarized in Table 1. The local IR luminosity function from *IRAS* sources (Sanders et al. 2003) is plotted for comparison.

For each luminosity bin the uncertainties, σ_ρ, were estimated using the Poisson statistics on the number of sources, so $\sigma_\rho = [\sum (1/V_{\rm max}^2)]^{1/2}$. Monte Carlo simulations were also performed to disentangle the uncertainties in the derivation of the luminosity function due to photometric errors. Each source was randomly given an IR luminosity within the uncertainty estimates and the luminosity function was recalculated. We find this adds between 0.03 and 0.09 dex to the luminosity function uncertainty, depending on the bin, but the Poisson statistics dominate the uncertainties.

We do not find any significant evolution in the sub-LIRG population ($L < 10^{11}\ L_\odot$) for the lowest redshift bin ($z < 0.4$) (Fig. 2). The high-redshift LFs show evidence for strong evolution of LIRGs and ULIRGs at $z > 0.4$.

TABLE 1

THE IR LUMINOSITY FUNCTIONS DERIVED FROM THE $1/V_{\rm max}$ ANALYSIS

$\log(L_{\rm IR}/L_\odot)$					
Low	High	Median	N	ρ(Mpc^{-3} logL^{-1})[a]	MONTE CARLO UNCERTAINTY[b] (dex)
$0.2 < z < 0.4$:					
10.20	10.50	10.44	7	$(3.36 \pm 1.58) \times 10^{-3}$	0.04
10.50	10.70	10.63	7	$(2.44 \pm 0.94) \times 10^{-3}$	0.06
$0.4 < z < 0.6$:					
10.60	10.90	10.81	9	$(1.77 \pm 0.65) \times 10^{-3}$	0.07
10.90	11.10	11.00	11	$(1.68 \pm 0.51) \times 10^{-3}$	0.09
11.10	11.30	11.24	9	$(1.24 \pm 0.41) \times 10^{-3}$	0.04
$0.6 < z < 0.9$:					
11.10	11.40	11.25	9	$(1.17 \pm 0.47) \times 10^{-3}$	0.05
11.40	11.70	11.47	13	$(7.90 \pm 2.31) \times 10^{-4}$	0.03
11.70	12.00	11.76	7	$(2.48 \pm 0.94) \times 10^{-4}$	0.07
$0.9 < z < 1.1$:					
11.50	11.70	11.67	8	$(1.44 \pm 0.55) \times 10^{-3}$	0.06
11.70	11.90	11.77	13	$(1.05 \pm 0.30) \times 10^{-3}$	0.07

[a] The errors quoted are Poisson uncertainties.

[b] This is the additional uncertainty to be added to the LF, calculated from Monte Carlo simulations of the uncertainty in the IR luminosity of each source. See § 4.2.

The IR LFs derived here are consistent with that derived from 24 μm (Le Floc'h et al. 2005) for the overlapping luminosity bins at $z < 1$. This implies that, on average, similar bolometric luminosities are derived from 24 and 70 μm for moderate-luminosity ($L < 10^{11.8}\ L_\odot$) and moderate-redshift sources ($z < 1$) sources. We cannot say whether this is the case for high luminosities and high redshifts (e.g., Chapman et al. 2005; Pope et al. 2006), as those sources are rare in the 70 μm data. Recent 70 μm stacking analysis of galaxies at $z \sim 2$ show that 24 μm observations at high redshift overestimate $L_{\rm IR}$ in comparison to 70 μm and other $L_{\rm IR}$ indicators (Daddi et al. 2007a, 2007b; Papovich et al. 2007).

To explore the evolution of IR sources we use the analytical form of the local LF from Sanders et al. (2003) that comprises a double power law: $\rho \propto L^{-0.6}$ for $\log(L/L_\odot) < 10.5$, $\rho \propto L^{-2.2}$ for $\log(L/L_\odot) > 10.5$. We assume that the evolving luminosity function can be described by $\rho(L, z) = g(z)\rho[L/f(z), 0]$. In this sense $g(z)$ and $f(z)$ describe the density and luminosity evolution of the LF, respectively. The commonly used form of evolution is to assume $f(z) = (1 + z)^p$ and $g(z) = (1 + z)^q$ (e.g., Condon 1984; Haarsma et al. 2000).

Using χ^2 minimization, we examine the best fit to the evolution of the IR LF. There is a well-known degeneracy between density and luminosity evolution. We find that the best-fit evolution parameters follow the relation $q = -2.19p + 6.09$. In the case of pure luminosity evolution ($q = 0$), we find $p = 2.78^{+0.34}_{-0.32}$.

These evolution constraints are broadly consistent with 24 μm studies that found $p = 3.2^{+0.7}_{-0.2}$ and $q = 0.7^{+0.2}_{-0.6}$ for the infrared luminosity function (Le Floc'h et al. 2005). Our results are also in good agreement with previous studies of IR sources (e.g., Franceschini et al. 2001).

Hopkins (2004) combined star formation rate data with faint radio source counts to find $p = 2.7 \pm 0.6$ and $q = 0.15 \pm 0.60$. If only pure luminosity evolution of radio sources is considered then $p = 2.5 \pm 0.5$ (Seymour et al. 2004) or $p = 2.7$ (Huynh et al. 2005). So our results are consistent with constraints on the evolution of the star-forming population from

deep radio surveys, indicating that the radio sources overlap with the ultradeep 70 μm population, as expected.

The constraints on the evolution of the IR LF can be used to determine the cosmic star formation rate (SFR) density. Using the calibration from Kennicutt (1998) and integrating over galaxies with $8.5 < \log(L/L_\odot) < 12.5$, we find that the SFR density at $z = 1$ is $0.15^{+0.04}_{-0.03}\ M_\odot\ \mathrm{yr}^{-1}\ \mathrm{Mpc}^{-3}$ for the best-fit pure luminosity evolution case. Here the uncertainties in SFR density do not include the systematics in the FIR/SFR calibration, which add about 0.3 dex to the absolute uncertainty. The SFR density derived here is lower than that estimated by the evolutionary models of Chary & Elbaz (2001) by about a factor of 1.7, but it is consistent with extinction corrected optical measures (e.g., Kewley et al. 2004) and 24 μm results (Le Floc'h et al. 2005).

The AGNs in our sample can be identified using the deep 2 Ms X-ray observations of GOODS-N (Alexander et al. 2003). Sources are classed as X-ray AGNs from X-ray band ratios, X-ray luminosity, and X-ray–to–optical flux ratios (Alexander et al. 2003; Bauer et al. 2004). At redshifts $z < 0.6$ we find only 7% of the 70 μm sources are X-ray AGNs, but this fraction increases to 27% for the $0.9 < z < 1.1$ redshift bin. The highest redshift LF in Figure 2 is contaminated by X-ray AGNs, but this does not significantly affect the evolution derived in this work.

5. CONCLUDING REMARKS

Based on ultradeep 70 μm observations of GOODS-N, and the spectroscopic and photometric redshifts available of galaxies in this well-studied field, we have derived luminosity functions for $z = 0.3$ to $z = 1.1$. We find strong evolution in galaxies with $L_{\mathrm{IR}} > 10^{11}\ L_\odot$ at redshifts $z > 0.4$. Assuming pure luminosity evolution of the form $(1 + z)^p$, we find $p = 2.78^{+0.34}_{-0.32}$. This confirms the strong evolution in LIRGs and ULIRGs between redshifts 0 and 1 that has been seen in previous work. The depth of the 70 μm data allows us to probe sub-LIRG luminosities, and we find little evolution in this population for $z \lesssim 0.4$. In the case of pure luminosity evolution, we find that the star formation rate density at $z = 1$ is $0.15^{+0.04}_{-0.03}\ M_\odot\ \mathrm{yr}^{-1}\ \mathrm{Mpc}^{-3}$.

This is the first result from an ultradeep FIR survey that reaches $z \sim 1$. However, we are limited by poor statistics—the number of bins available for the LF at each redshift is limited by the small number of cataloged sources. The area covered is only $10' \times 18'$, so these results are also affected by cosmic variance.

The Far Infrared Deep Extragalactic Legacy (FIDEL) *Spitzer* legacy project, currently underway, will cover the extended Chandra Deep Field–South and the extended Groth strip at 70 μm with depths similar to those of the GOODS-N. The total area covered will be about 9 times that used in this work, and the FIDEL project will detect over 1000 LIRGs at moderate redshift. So in the near future, large ultradeep FIR surveys such as FIDEL will enable even more detailed studies of the FIR luminosity function and the evolution of infrared galaxies.

This work is based on observations made with the *Spitzer Space Telescope*, which is operated by the Jet Propulsion Laboratory, California Institute of Technology, under a contract with NASA. Support for this work was provided by NASA through an award issued by JPL/Caltech.

REFERENCES

Alexander, D. M., et al. 2003, AJ, 126, 539
Bauer, F. E., Alexander, D. M., Brandt, W. N., Schneider, D. P., Treister, E., Hornschemeier, A. E., & Garmire, G. P. 2004, AJ, 128, 2048
Blain, A. W., Smail, I., Ivison, R. J., Kneib, J.-P., & Frayer, D. T. 2002, Phys. Rep., 369, 111
Chapman, S. C., Blain, A. W., Smail, I., & Ivison, R. J. 2005, ApJ, 622, 772
Chary, R., & Elbaz, D. 2001, ApJ, 556, 562
Chary, R., et al. 2004, ApJS, 154, 80
Cohen, J. G., Hogg, D. W., Blandford, R., Cowie, L. L., Hu, E., Songaila, A., Shopbell, P., & Richberg, K. 2000, ApJ, 538, 29
Condon, J. J. 1984, ApJ, 284, 44
Daddi, E., et al. 2007a, preprint (arXiv:0705.2831)
———. 2007b, preprint (arXiv:0705:2832)
Dale, D. A., & Helou, G. 2002, ApJ, 576, 159
Dale, D. A., et al. 2005, ApJ, 633, 857
Elbaz, D., Cesarsky, C. J., Chanial, P., Aussel, H., Franceschini, A., Fadda, D., & Chary, R. R. 2002, A&A, 384, 848
Franceschini, A., Aussel, H., Cesarsky, C. J., Elbaz, D., & Fadda, D. 2001, A&A, 378, 1
Frayer, D. T., et al. 2006a, AJ, 131, 250
———. 2006b, ApJ, 647, L9
Giavalisco, M., et al. 2004, ApJ, 600, L93
Haarsma, D. B., Partridge, R. B., Windhorst, R. A., & Richards, E. A. 2000, ApJ, 544, 641
Hopkins, A. M. 2004, ApJ, 615, 209
Huynh, M. T., Jackson, C. A., Norris, R. P., & Prandoni, I. 2005, AJ, 130, 1373
Huynh, M. T., Pope, A., Frayer, D. T., & Scott, D. 2007, ApJ, 659, 305
Kennicutt, R. C., Jr. 1998, ARA&A, 36, 189
Kewley, L. J., Geller, M. J., & Jansen, R. A. 2004, AJ, 127, 2002
Lagache, G., Dole, H., & Puget, J.-L. 2003, MNRAS, 338, 555
Le Floc'h, E., et al. 2005, ApJ, 632, 169
Mobasher, B., et al. 2007, ApJS, 172, 117
Papovich, C., et al. 2004, ApJS, 154, 70
———. 2007, ApJ, in press (arXiv:0706.2164)
Pérez-González, P. G., et al. 2005, ApJ, 630, 82
Pope, A., et al. 2006, MNRAS, 370, 1185
Sanders, D. B., Mazzarella, J. M., Kim, D.-C., Surace, J. A., & Soifer, B. T. 2003, AJ, 126, 1607
Schmidt, M. 1968, ApJ, 151, 393
Serjeant, S., et al. 2004, MNRAS, 355, 813
Seymour, N., McHardy, I. M., & Gunn, K. F. 2004, MNRAS, 352, 131
Takeuchi, T. T., Ishii, T. T., Dole, H., Dennefeld, M., Lagache, G., & Puget, J.-L. 2006, A&A, 448, 525
Wirth, G. D., et al. 2004, AJ, 127, 3121
Yun, M. S., Reddy, N. A., & Condon, J. J. 2001, ApJ, 554, 803